Electrochemical and Spectroscopic Studies on the Interaction Modes of Calf Thymus DNA with Antibacterial Schiff Bases obtained from Substituted Salicylaldehydes and Sulfamethizole

Vahide Pehlivan[1], Ender Biçer[1,*], Yeliz Genç Bekiroğlu[2], Necmi Dege[3]

[1] Department of Chemistry, Faculty of Arts and Sciences, Ondokuz Mayıs University, 55139 Atakum-Samsun, TURKEY
[2] Department of Herbal and Animal Production, Bafra Vocational School, Ondokuz Mayıs University, 55400 Bafra-Samsun, TURKEY
[3] Department of Physics, Faculty of Arts and Sciences, Ondokuz Mayıs University, 55139 Atakum-Samsun, TURKEY
[*]E-mail: ebicer@omu.edu.tr

In this study, two Schiff bases have been prepared from the condensation of sulfamethizole (SMTZ) with 3-methoxy and 5-nitro derivatives of salicylaldehyde. These compounds have been characterized by elemental analysis, FT-IR, UV-Vis, ^{1}H-NMR, melting point and X-ray measurements. The *in vitro* anti-bacterial properties of these Schiff bases against various microorganisms (*E. coli* ATCC 25922, *S. aureus* ATCC 25923 and trimethoprim sulfamethoxazole resistant clinical isolate *E. coli* (*SXT-R E. coli*)) have been also investigated. The Schiff base with -NO_2 (Schiff base B, MIC: 0.5 μg mL^{-1}) shows stronger antibacterial activity than SMTZ, other reactive compounds and the Schiff base with -OCH_3 (Schiff base A) against *S. aureus* ATCC 25923. The interaction of the Schiff bases with calf thymus DNA (CT-DNA) in the physiological pH (7.4) was studied by electrochemical and spectroscopic methods. The electrochemical and spectroscopic data revealed that Schiff bases bind to CT-DNA in 1:1 stoichiometry. The binding affinity followed the order Schiff base A > Schiff base B. It has been found that the binding affinity orders determined from different methods are in good agreement with each other. The obtained results indicate that Schiff base A binds to CT-DNA by means of electrostatic forces; however, Schiff base B could interact with CT-DNA molecule by intercalative mode.

Keywords: Antimicrobial activity, DNA interaction, Schiff bases, Substituted salicylaldehydes, Sulfamethizole.

1. INTRODUCTION

Bacteria that are highly resistant to antibiotics can cause delayed treatment and even fatal effects in infectious diseases [1]. Therefore the synthesis of new antibacterials is very important for the effective treatments.

The binding of DNA with pharmaceutical active compounds is very important to determine the action mechanism of DNA-targeted drugs in the life sciences and drug design process [2,3]. It is well known that the effective binding modes between small molecules and DNA can be given as two main groups: covalent binding and non-covalent binding, including non-specific electrostatic interaction, intercalative and DNA major/minor groove bindings [2]. Non-covalent binding is the most effective binding mode for small molecules [2]. Non covalent interactions are intercalative, groove binding or electrostatic interactions [4]. At the covalent binding, a labile ligand is replaced by a nitrogen atom of DNA bases [2,4].

It was reported that Schiff bases showed a broad range of biological activities, including antifungal, antibacterial, antimalarial, antiproliferative, anti-inflammatory, antiviral, and antipyretic properties [5-7]. The investigations on the interaction of Schiff bases with DNA are important for the seeking and design of new drugs [8,9].

The sulfonamides are pharmacologically active compounds to be widely used to treat the various human and animal infections [10]. On the other hand, many aldehydes are known to be potential inhibitors for DNA synthesis [11]. It was also indicated that the sulfonamide-azomethine compounds which are resulted from the reaction of salicylaldehyde and benzaldehyde with sulfonamide may show enhanced biological activity [11]. Therefore the synthesis of Schiff bases derivated from the sulfonamides and the Schiff base-DNA interactions were the subject of many studies [11-45].

SMTZ (Scheme 1) is a sulfonamide class antibiotic [46] and used in the treatment of the urinary tract infections [47]. This paper mainly presents both CT-DNA interactions at physiological pH and antibacterial activity of Schiff bases which are resulted from the condensation of substituted salicylaldehydes with SMTZ.

2. EXPERIMENTAL

2.1. Apparatus

EG&G PAR 384B Polarographic Analyzer coupled with EG&G PARC 303A stand and driven by ECDSOFT [48] software was employed for voltammetric experiments at room temperature. The three-electrode system was consisted of $Ag|AgCl|KCl_{sat.}$ as reference electrode, Pt wire as counter electrode and hanging mercury drop electrode (HMDE) as working electrode. Nitrogen gas was purged to get rid of the dissolved oxygen from the solution before every voltammetric measurements. Jenway 3010 pH-meter was used for the pH measurements.

Electronic spectra of the Schiff bases were recorded in the range of 200 -800 nm using Thermo Scientific Evolution Array EA-1301005 UV-Vis. spectrometer. The FT-IR spectra in the 4000–650 cm^{-1} range were recorded with a Bruker Vertex 80V spectrophotometer.

The elemental analysis was performed using a LECO, CHNS-932 analyzer and the ^{1}H NMR spectra of Schiff bases in DMSO-d$_6$ were recorded on Bruker Biospin spectrometer (300 MHz) using Tetramethylsilane (TMS) as internal standard at Middle East Technical University (METU) Central Laboratory (Ankara, Turkey). Melting points of the Schiff bases were determined on a Stuart Melting Point SMP 30 apparatus.

2.2. Reagents

3-methoxy salicylaldehyde and 5-nitro salicylaldehyde were obtained from Merck. SMTZ was purchased from Sigma-Aldrich (purity %99) and used without further purification. CT-DNA was bought from Sigma Aldrich. All other chemicals were of analytical grade and used without any further purification. The stock solutions of Schiff bases were prepared daily by dissolution in hot methanol and then were further diluted with the same solvent to appropriate concentration. Other solutions were prepared in deionized ultra pure water (specific resistivity = 18.2 MΩ cm), obtained from MINI PURE DEST-UP Water Purification system. 0.02 M phosphate buffer (pH 7.4) was prepared from 0.5 M H$_3$PO$_4$ solution and also adjusted to the desired pH value with 0.5 M NaOH solution.

2.3. CT-DNA solution

The stock solution of CT-DNA was prepared by dissolving an appropriate amount (1×10^{-3} g) of DNA in ultra pure water (50 mL) and stored at 4 °C. According to the described method in the literature [49], its concentration (2.5×10^{-4} M) was determined by means of the absorbance value at 260 nm using a molar absorption coefficient (ε$_{260}$), 6600 M^{-1} cm^{-1}. The purity of CT-DNA was controlled by the ratio of the absorbance at 260 nm to that at 280 nm (A$_{260}$/A$_{280}$) [50]. Due to this ratio > 1.8, it was thought that DNA was sufficiently free from protein [50].

2.4. Synthesis and characterization of Schiff bases

In order to synthesis the Schiff bases, the substituted salicylaldehydes (3-methoxy salicylaldehyde (3-MeOC$_6$H$_3$(OH)CHO (abbreviated as 3-MSA) and 5-nitro salicylaldehyde (5-NO$_2$C$_6$H$_3$(OH)CHO) (abbreviated as 5-NSA)) were used and their reactions were performed with SMTZ as given in Scheme 1. The mixtures were refluxed for 4-5 h with continuous stirring in methanol at 70-80 °C (Scheme 1). The solutions were cooled up to room temperature after the completion of the reactions. Thus, the precipitate obtained was filtered off, washed several times with cold methanol and dried. The obtained Schiff bases were crystallized in acetonitrile.
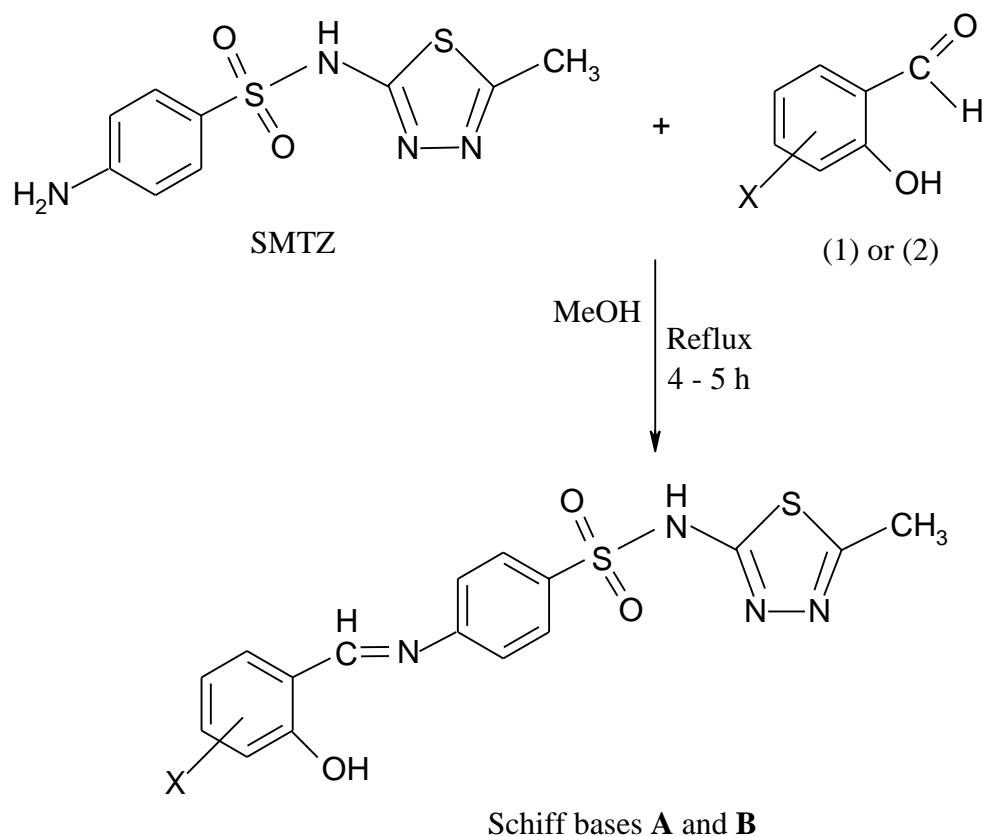
Scheme 1. Schematic representation of the preparation of Schiff bases **A** and **B** (**X**: 3-OCH$_3$ (**A**), 5-NO$_2$ (**B**)) **A**: E-4-(2-hydroxy-3-metoxy benzylidine amino)-N-(5-methyl-3,4-thiazol-2-yl) benzene sulphonamide **B**: E-4-(2-hydroxy-5-nitro benzylidine amino)-N-(5-methyl-3,4-thiazol-2-yl) benzene sulphonamide

Schiff base A, yield: 86% (m.p. 227-228 °C); CHNS analysis: found % C, 50.40; H, 4.08; N, 13.86; S, 15.95; Calc. % C, 50.48; H, 3.99; N, 13.85; S, 15.86. ^{1}H NMR (TMS, DMSO-d$_6$) δ ppm: 2.4 (methyl proton, C-CH$_3$), 3.8 (-O-CH$_3$), 6.5 – 8.1 (multiplet, the aromatic ring protons), 9.0 (s, –CH=N), 10.3 (s, phenolic protons at *o*-position of the azomethine group) and 12.7 (br s, 1H, SO$_2$-NH-). FT-IR bands (v in cm^{-1}): 3159 v (N-H str), 3028 v (C-H aromatic), 2810 v (CH, saturated), 1619, 1557 v (-C=N-), 1249 v (C–O), 1318 v_a (SO$_2$), 1153 v_s (SO$_2$), 919 v (S–N) and 842 v (C–S). Electronic spectra (λ_{max} / nm in MeOH solvent): 223, 267, 288 (π → π*) and 318 (n → π*).

Schiff base B, yield: 81% (m.p. 268-269 °C); CHNS analysis: found % C, 45.61; H, 3.45; N, 16.69; S, 15.31; Calc. % C, 45.82; H, 3.12; N, 16.69; S, 15.29. ^{1}H NMR, (TMS, DMSO-d$_6$) δ ppm: 2.4 (methyl proton, C-CH$_3$), 6.5 – 8.9 (multiplet, the aromatic ring protons), 9.1 (s, –CH=N), 10.3 (s, phenolic protons at *o*-position of the azomethine group) and 11.9 (br s, 1H, SO$_2$-NH-). FT-IR bands (v in cm^{-1}): 3141 v (N-H str), 3025 v (C-H aromatic), 2878 v (C-H alkanes), 1620, 1531 v (-C=N-), 1227 v (C–O), 1341 v_a (SO$_2$), 1154 v_s (SO$_2$), 1282 v_s (NO$_2$), 1481 v_a (NO$_2$), 919 v (S–N) and 836 v (C–S). Electronic spectra (λ_{max} / nm in MeOH solvent): 264 (π → π*), 360 and 419 (n → π*).

2.4.1. X-ray Crystallography

The proper single crystals of Schiff bases A and B were used for X-ray measurements. The single-crystal X-ray data were collected on a STOE IPDS II image plate diffractometer at 296 K. Graphite-monochromated Mo Ka radiation (λ = 0.71073 Å) and the w-scan technique were used. Crystal structures of the two compounds were solved by direct method. All non-hydrogen atoms were refined anisotropically. All calculations were performed using X-AREA [51], X-RED32 [51], SHELXT [52], SHELXL2016/6 [53], ORTEP-3 for Windows [54], WinGX [54] and PLATON [55]. Crystal data and refinement parameters are given in Table 1. In addition, the geometrical parameters for hydrogen bonds are shown in Table 2.

Table 1. Crystal Data and Refinement Parameters for the Schiff bases A and B

| Compound	**Schiff base A**	**Schiff base B**
Empirical formula	$C_{17}H_{16}N_4O_4S_2$	$C_{16}H_{13}N_5O_5S_2$
Molecular weight	404.46	419.43
Crystal color, habit	Yellow, Prism	Orange, Prism
Crystal size (mm^3)	$0.46 \times 0.27 \times 0.11$	$0.26 \times 0.22 \times 0.19$
Crystal system	Monoclinic	Triclinic
Space group	$P21/c$	$P\bar{1}$
a (Å)	5.3997 (2)	6.4905 (11)
b (Å)	10.2492 (4)	9.2016 (13)
c (Å)	32.5025 (14)	15.928 (2)
α (°)	90	86.519 (11)
β (°)	90.439 (3)	79.237 (12)
γ (°)	90	70.758 (12)
V (Å^3)	1798.72 (12)	882.3 (2)
Z	4	2
D_{calc} (g cm^{-3})	1.494	1.579
Absorption coefficient (μ, mm^{-1})	0.33	0.34
θ range collected (°)	1.9–27.3	1.3–27.0
T_{min} and T_{max}	0.882 and 0.969	0.923 and 0.963
No. of measured, independent and observed [$I > 2\sigma(I)$] reflections	13459, 3813 and 2787	7311, 3074 and 1486
R_{int}	0.044	0.080
$(\sin \theta/\lambda)$max (Å^{-1})	0.634	0.596
$R[F^2 > 2\sigma(F^2)]$, $wR(F^2)$, S	0.040, 0.112, 1.04	0.115, 0.348, 1.07
No. of parameters	247	255
No. of restraints	6	0
H-atom treatment	H-atom parameters constrained	H-atom parameters constrained
$\Delta\rho_{max}$, $\Delta\rho_{min}$ (e Å^{-3})	0.55, −0.55	0.64, −0.40

Table 2. Geometrical Parameters for Hydrogen Bonds

D—H···A	D–H (Å)	H···A (Å)	D···A (Å)	D–H···A (°)
Schiff base A				
O3—H3···N4	0.82	1.93	2.651 (3)	146
N2—H2···N3[i]	0.86	2.05	2.904 (2)	170
C1—H1B···N1[ii]	0.96	2.56	3.507 (3)	168
Schiff base B				
O3—H3···N4	0.82	2.17	2.607 (8)	114
N2—H2···N3[i]	0.86	2.11	2.955 (14)	168
C8—H8···O5[ii]	0.93	2.60	3.184 (11)	122

Symmetry transformation used to generate the symmetry related atoms: (i) −x+1, −y+1, −z+1; (ii) −x+1, −y, −z+1 (for Schiff base A); (i) −x+1, −y+1, −z+2; (ii) −x+1, −y+2, −z+1 (for Schiff base B).

2.4.2. Structure Description of the Schiff bases

The molecular structures of Schiff bases A and B are given in Figures 1 and 2, respectively.
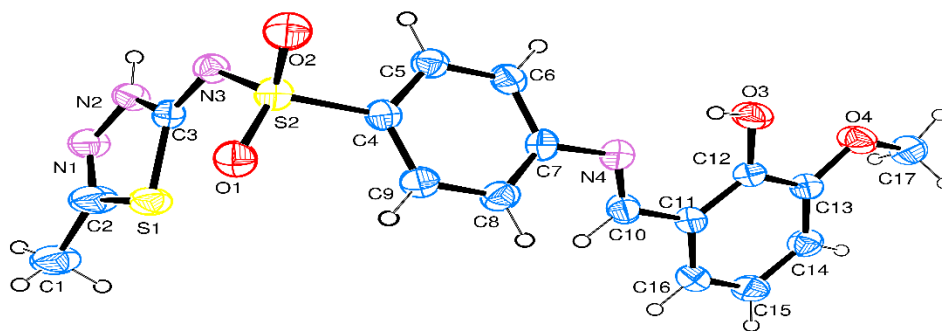
Figure 1. ORTEP view of Schiff base A with thermal ellipsoids (30% probability level).
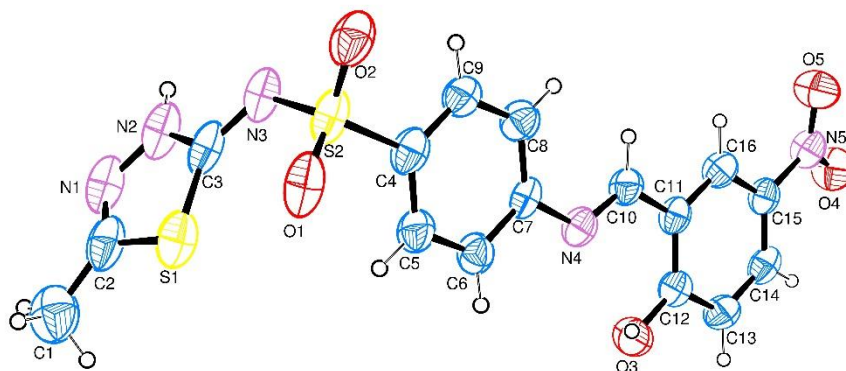
Figure 2. ORTEP view of Schiff base B with thermal ellipsoids (50% probability level).

2.5. In vitro antimicrobial assay

Minimum Inhibitor Concentration (MIC) method was used against Gram-positive and Gram-negative samples to determine the antimicrobial activities of newly synthesized substances in line with the directives of Clinical and Laboratory Standards Institute (CLSI) [56]. *Escherichia coli* ATCC 25922, *Staphylococcus aureus* ATCC 25923 standard strains and Trimethoprim/Sulphamethoxazole (1.25/23.75 µg^{-1}-Bactrim) resistant clinical isolate *E. coli* strain (SXT-R *E. coli*) were used as microorganisms in this study. SMTZ was used as control compound.

3. RESULTS AND DISCUSSION

3.1. In vitro antimicrobial activities of Schiff bases A and B

In vitro antibacterial activities of the Schiff bases A and B, SMTZ and other reactive compounds have been also studied against the gram-positive and gram-negative bacteria and clinical isolate *E. coli.*

MIC values of all the tested substances against *E. coli* were found to be 8 µg mL^{-1} (Table 3). It is remarkable for clinical isolate *E. coli* to have MIC values of 8 µg mL^{-1} against all test compounds while it was resistant against Trimethoprim/Sulphamethoxazole which had 1.25/23.75 µg^{-1} substance content. While Schiff base B showed 0.5 µg mL^{-1} MIC value against *Staphylococcus aureus* bacteria, all the other compounds showed 4 µg mL^{-1} MIC value. Consequently, the antibacterial activity of Schiff base B is more effective than that of both SMZ and Schiff base A. According to the Schiff bases (A and B), this result might be sourced from the presence of nitro group. The synthesis of Schiff bases derivated from sulphonamides may play an important role to design the potential antibacterial agents.

Table 3. Minimum inhibitory concentration (MIC) of Schiff bases (**A** and **B**) and other reactive compounds

Compounds	MIC (µg mL^{-1})		
	Gram positive	Gram negative	
	S. aureus ATCC 25923	*E. coli* ATCC 25922	SXT-R *E. coli*[*]
Schiff base A	4	8	8
Schiff base B	0.5	8	8
3-MSA	4	8	8
5-NSA	4	8	8
SMTZ	4	8	8

*: Trimethoprim/Sulphamethoxazole (1.25/23.75 µg^{-1} Bactrim) resistant clinical isolate strain

3.2. Voltammetric behaviours of Schiff bases A and B

Electrochemical behaviours of Schiff bases A and B in B-R buffer (pH 7.4) were studied by means of SWV and CV techniques. The square-wave voltammograms of Schiff bases A and B are

given in Fig. 3. As can be seen in Fig. 3, Schiff base A shows three cathodic peaks at −0.352, −1.240 and −1.584 V, respectively. According to the literature data, these peaks can be attributed to the reduction of the Hg(I)-Schiff base A complex which adsorbs at electrode surface, the reduction of azomethine group (>C=N−) and the catalytic hydrogen reduction, respectively [57-62]. However, Schiff base B exhibits four cathodic peaks at −0.232, −0.876, −1.232 and −1.460 V, respectively (Fig. 4). As different from the Schiff base A, the peak at −0.876 V can be assigned to the reduction of nitro group [63-65]. Other peaks have the similar assignments with those given for Schiff base A, respectively.
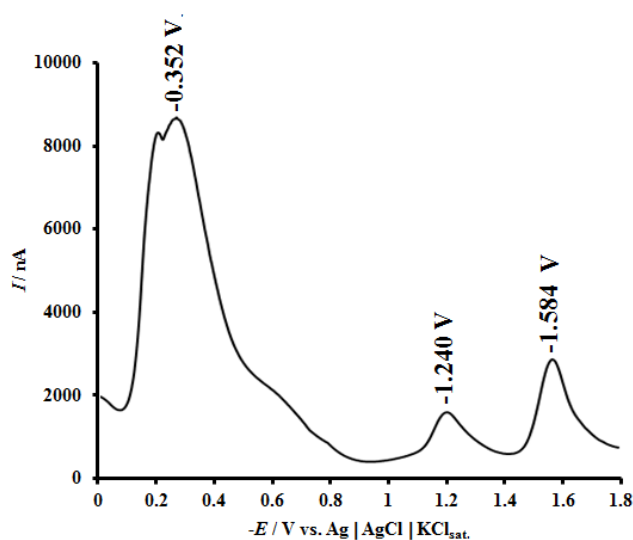

Figure 3. Square-wave voltammogram of 1.67×10^{-4} M Schiff base A at 0.02 M phosphate buffer (pH=7.4). (*Other experimental conditions*: scan rate, 200 mVs^{-1}; drop size, medium and equilibrium time, 5 s).
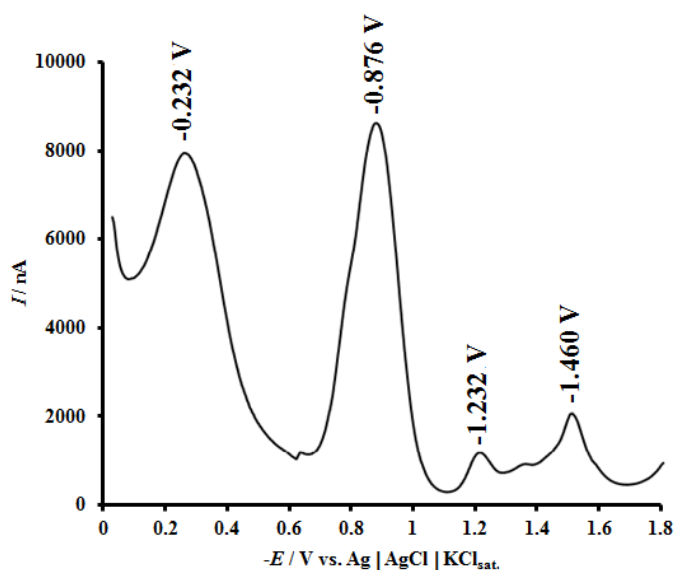

Figure 4. Square-wave voltammogram of 9.1×10^{-5} M Schiff base B at 0.02 M phosphate buffer (pH=7.4) (*Other experimental conditions* are as described in Fig. 3).

3.3. Interaction of Schiff bases A and B with CT-DNA

3.3.1. Voltammetry

Interaction of Schiff bases A and B with CT-DNA in physiological pH (7.4) was studied using cyclic voltammetry. For the interaction studies, the major cathodic peaks of Schiff bases A and B at −1.240 and −0.892 V, respectively, were selected. When CT-DNA was added to the cell including Schiff bases A or B, the currents of main peaks decreased and their peak potentials shifted to more negative or positive values owing to the interactions (Figs. 5 and 6). The decrease in the peak current resulted from the decrease in free Schiff base concentration due the formation of the Schiff base-DNA adducts. In the presence of CT-DNA, the main peak of Schiff base A has the negative peak potential shift of 25 mV while the positive shift at the major peak of Schiff base B is 37 mV.
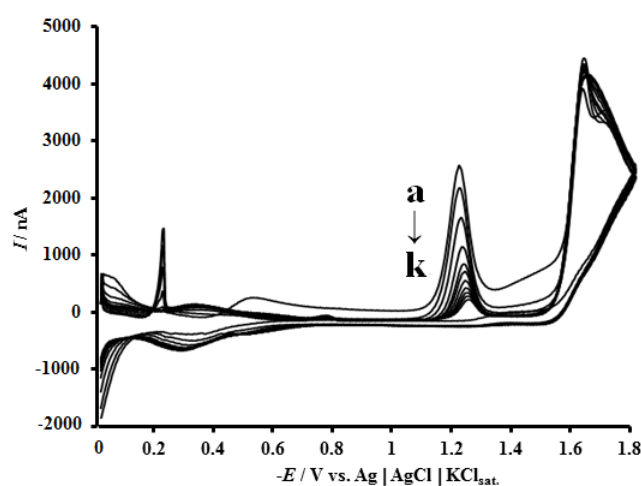

Figure 5. Cyclic voltammograms of 1.6×10^{-4} M Schiff base A at phosphate buffer (pH=7.4) in the absence (a) and presence of (b) 1.05×10^{-7}, (c) 2.10×10^{-7}, (d) 3.14×10^{-7}, (e) 4.16×10^{-7}, (f) 5.18×10^{-7}, (g) 6.20×10^{-7}, (h) 7.20×10^{-7}, (i) 8.20×10^{-7}, (j) 9.20×10^{-7}, (k) 1.02×10^{-6} M CT-DNA. (*Other experimental conditions*: scan rate, 500 mVs^{-1}; drop size, medium and equilibrium time, 5 s).
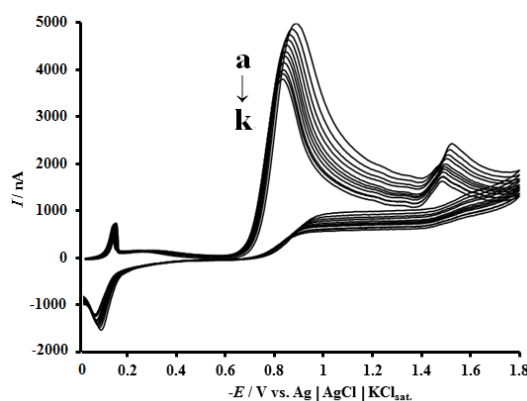

Figure 6. Cyclic voltammograms of 9.1×10^{-5} M Schiff base B at phosphate buffer (pH=7.4) in the absence (a) and presence of (b) 1.95×10^{-6}, (c) 3.63×10^{-6}, (d) 5.08×10^{-6}, (e) 6.35×10^{-5}, (f) 7.47×10^{-6}, (g) 8.47×10^{-6}, (h) 9.36×10^{-6}, (i) 1.02×10^{-5}, (j) 1.08×10^{-5}, (k) 1.15×10^{-5} M CT-DNA. (*Other experimental conditions* are as described in Fig. 5).

According to the shifting sides at these main peak potentials, it can be said that the Schiff base B intercalates into double helix of CT-DNA (for hydrophobic interactions); however, the binding of Schiff base A with CT-DNA has an electrostatic interaction character [66-69].

It was reported that the intercalative and groove bindings are related with the grooves in the DNA double helix while the electrostatic binding can take place out of the groove or on the surface of the DNA molecule [70].

Laviron's equation (Eq. 1) was used to evaluate the kinetic constants of electrode reaction in the absence and presence of CT-DNA [10, 71].

$$E_p = E^{0'} + (RT / (\alpha nF)) [\ln [(RTk_s^0) / (\alpha nF)] - \ln v] \tag{1}$$

Where α is the electron transfer coefficient, k_s^0 is the standard heterogeneous rate constant, v the scan rate, $E^{0'}$ is the formal potential and n is the electron transfer number [10, 71]. According to Eq. 1, if the $E^{0'}$ is known and also E_p is linear with $\ln v$, αn and k_s^0 values can be calculated from the slope and intercept, respectively. From the plot of E_p *vs.* v, the $E^{0'}$ value may be determined by extrapolating the line to $v = 0$. So, the electrochemical parameters of the Schiff bases and their CT-DNA reaction solutions were calculated (Table 4).

Table 4. The electrochemical parameters obtained from CV data

	$E^{0'}$ (V)	αn	k_s^0 (s^{-1})
Schiff base A	−1.200	1.232	2.825
Schiff base A + CT-DNA	−1.230	1.395	3.110
Schiff base B	−0.860	0.840	3.460
Schiff base B + CT-DNA	−0.837	0.870	3.933

As can be seen in Table 4, the electrochemical parameters of Schiff bases in the presence of CT-DNA, have varied obviously. These changes at the electrochemical parameters after adding CT-DNA verified that Schiff bases A and B not only took place interaction with CT-DNA [72] but also formed the electrochemical active complexes [73]. As similar to the changes at E_p values, the shifts at $E^{0'}$ could also indicate the interaction mode of Schiff bases with CT-DNA [74-76]. The $E^{0'}$ of Schiff base A in the presence of CT-DNA shifts to more negative potential by 30 mV (Table 4), suggesting an electrostatic interaction of Schiff base A with CT-DNA. However, the $E^{0'}$ of Schiff base B in the presence of CT-DNA shifted to more positive potential by 23 mV (Table 4), also revealing that Schiff base B intercalated into CT-DNA. The decrease of the main reductive peak currents may be resulted from the surrounding of the electroactive -NO$_2$ and >C=N moieties of Schiff bases by the helix of CT-DNA, decreasing diffusion coefficients of the complexes with large molecular weights and prevention of reduction [4].

3.3.1.1. The salt effect on the interaction

To explain the interaction mode, the effect of ionic strength was studied by the addition of 0.0041 - 0.0320 M NaCl into the Schiff bases and CT-DNA mixed solutions. Figs. 7 and 8 showed that NaCl concentration has different effects on the interactions. The main peak current of Schiff base A in the presence of CT-DNA strongly decreased with the increase of NaCl concentration and nearly weakened to 83.3% of that in the absence of NaCl when the ionic strength reaches 32 mM (Fig. 7), which indicated that the interaction between Schiff base A and CT-DNA was mainly caused by electrostatic attraction [77].
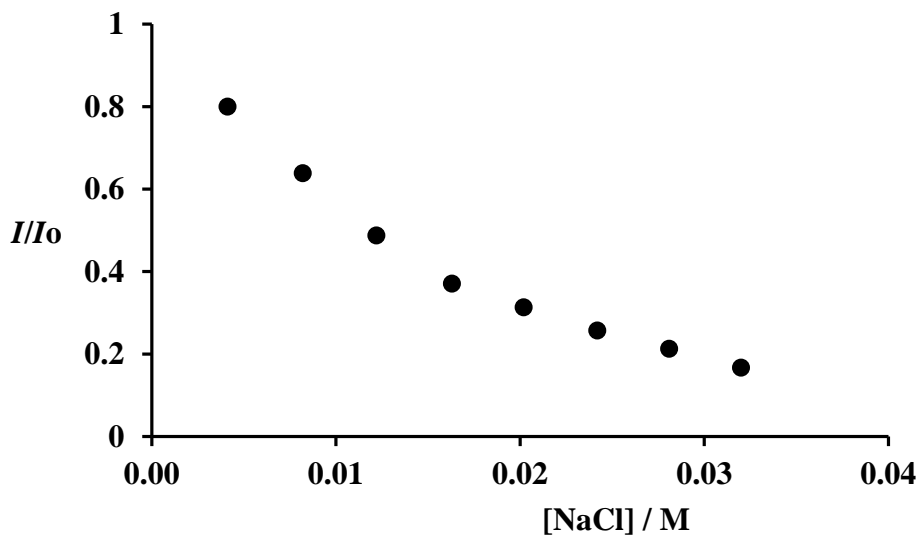

Figure 7. The plot of I/I_0 *versus* NaCl concentration for the peak of Schiff base A at -1.240 V. *Experimental conditions:* 1.60×10^{-4} M Schiff base A and 2.03×10^{-7} M CT-DNA in 0.02 M phosphate buffer (pH 7.4). I_0 and I are the peak current values in the absence and presence of NaCl, respectively. (*Other experimental conditions* are as described in Fig. 5).
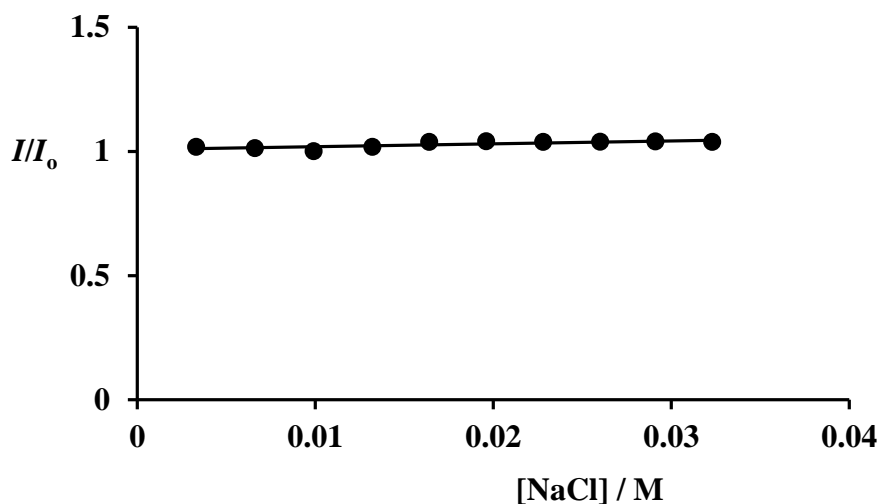

Figure 8. The plot of I/I_0 *versus* NaCl concentration for the peak of Schiff base B at -0.892 V. *Experimental conditions:* 1.29×10^{-4} M Schiff base B and 4.92×10^{-6} M CT-DNA in 0.02 M phosphate buffer (pH 7.4). I_0 and I are the peak current values in the absence and presence of NaCl, respectively. (*Other experimental conditions* are as described in Fig. 5).

By contrast, the increasing ionic strength did not nearly change the current of main reduction peak in the Schiff base B and CT-DNA system (Fig. 8). This result showed that the interaction of Schiff base B with CT-DNA is independent on salt concentration and was an intercalative manner [78]. Already, the effect of ionic strength on the DNA interactions and the determination of interaction modes were clearly explained by Shah et al [79].

3.3.2. UV-Visible Spectroscopy

The interactions of Schiff bases A and B with CT-DNA were also studied by UV–vis. absorption titration for getting further information about their interactions and binding strengths. The effect of CT-DNA concentration on the electronic absorption spectra of Schiff bases A and B are shown in Figs. 9 and 10. With increasing CT-DNA concentration, the absorbance values of maximum absorption bands of Schiff bases A and B decreased (hypochromic effect). The hypochromism of about 85% was observed for Schiff base A at 260 nm) whereas it was 90% for Schiff base B at 258 nm. In the presence of CT-DNA, the maximum absorption wavelength of Schiff base A didn't shift, however that of Schiff base B has the blue-shift of 2 nm. From the aforementioned results, it can be concluded that the binding mode between Schiff base B and CT-DNA is a typical characteristic of intercalation, but the interaction of Schiff base A with CT-DNA confirms an electrostatic binding mode [66,80]. So, for the binding modes of Schiff bases A and B with CT-DNA, the spectroscopic results are agreed with the electrochemical conclusions.
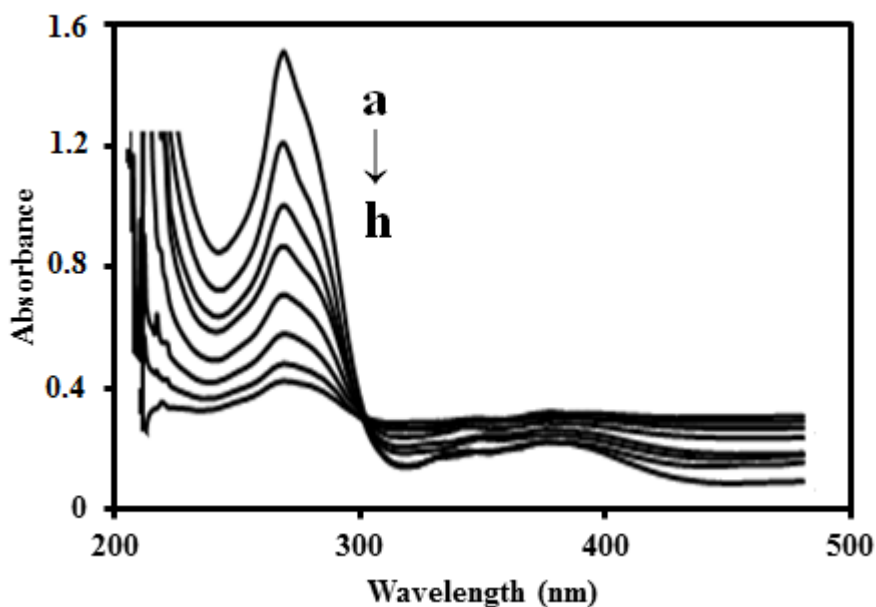

Figure 9. UV-Vis spectra of 8.34×10^{-5} M Schiff base A at phosphate buffer (pH=7.4) in the absence (a) and presence of (b) 2.08×10^{-7}, (c) 3.03×10^{-7}, (d) 6.36×10^{-7}, (e) 8.46×10^{-7}, (f) 1.06×10^{-6}, (g) 1.27×10^{-6}, (h) 1.48×10^{-6} M CT-DNA.
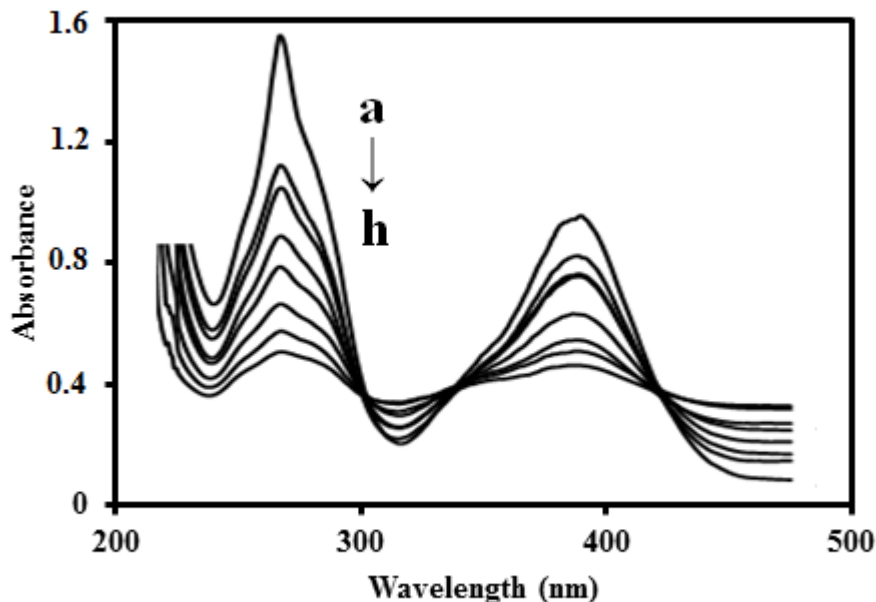
Figure 10. UV-Vis spectra of 4.17×10^{-4} M Schiff base B at phosphate buffer (pH=7.4) in the absence (a) and presence of (b) 1.04×10^{-6}, (c) 2.12×10^{-6}, (d) 3.18×10^{-6}, (e) 4.23×10^{-6}, (f) 5.29×10^{-6}, (g) 6.35×10^{-6}, (h) 7.41×10^{-6} M CT-DNA.
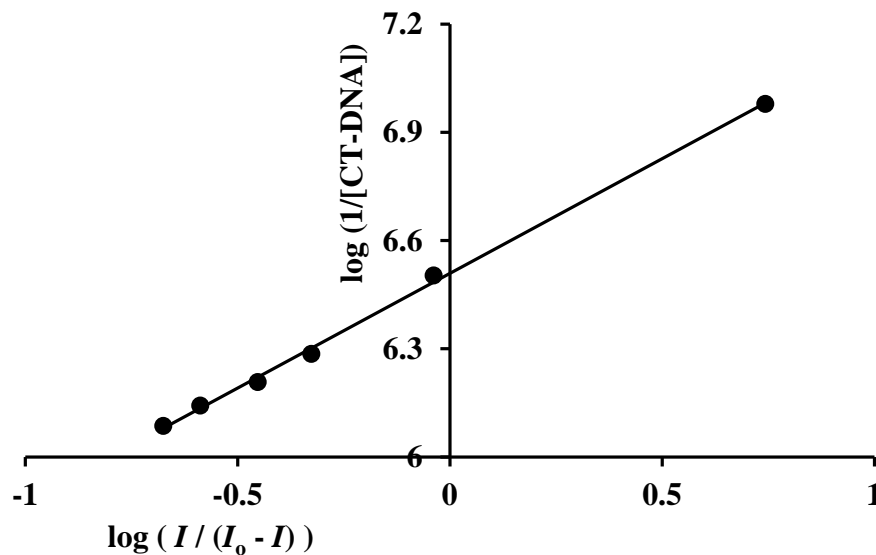
3.3.3. Binding Constant and Stoichiometry

Figure 11. The plot of log (1/[CT-DNA]) *versus* log ($I / (I_0 - I)$) for Schiff base A. *Experimental conditions:* 1.6×10^{-4} M Schiff base A in 0.02 M phosphate buffer (pH 7.4).

According to voltammetric data, the binding constants of 1:1 Schiff base-CT-DNA association complexes was determined using following equation 2 [81]:

$$\log (1 / [CT\text{-}DNA]) = \log K + \log (I / (I_0 - I)) \qquad (2)$$

Where, K is the binding constant, I and I_0 are the main peak currents of the Schiff bases in the presence and absence of CT-DNA, respectively. As the slopes of the straight-lines in Fig. 11 and 12 are less than unity, it can be assumed that the stoichiometry of Schiff base-CT-DNA complexes is 1:1. According to the Eq. 2, from the intercepts of the plots of $\log (1/[CT\text{-}DNA])$ *versus* $\log (I/(I_0 - I))$, K values were determined (Table 5).
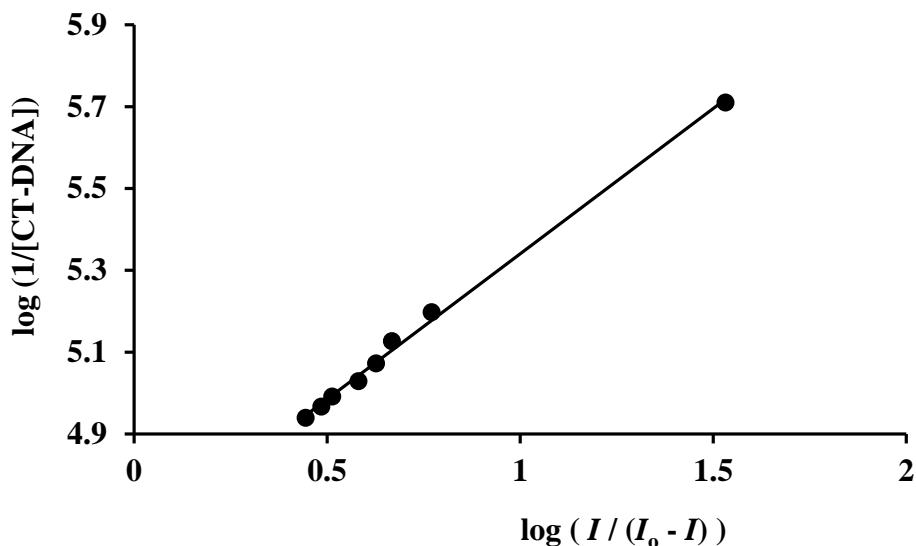

Figure 12. The plot of $\log (1/[CT\text{-}DNA])$ *versus* $\log (I / (I_0 - I))$ for Schiff base B. *Experimental conditions:* 9.1×10^{-5} M Schiff base B in 0.02 M phosphate buffer (pH 7.4).

Table 5. The binding constants calculated from CV and UV-Vis. Data

	$K\,(\mathrm{M}^{-1})$	
	CV	*UV-Vis.*
Schiff base A + CT-DNA	2.462×10^{6}	9.853×10^{5}
Schiff base B + CT-DNA	4.259×10^{4}	3.811×10^{5}

Assuming the most common host–guest ratio of 1:1, the data of UV–vis. absorption titration was also used to determine the binding constant (K) using the equation 3 as given below [66]:

$$[A_0/(A - A_0)] = [\varepsilon_G / (\varepsilon_{H\text{-}G} - \varepsilon_G)] + [\varepsilon_G / (\varepsilon_{H\text{-}G} - \varepsilon_G)] \times (1 / K [CT\text{-}DNA]) \qquad (3)$$

where A_0 and A are the absorbances of Schiff base at 260 or 258 nm in the absence and presence of CT-DNA, and ε_G and $\varepsilon_{H\text{-}G}$ are their absorption coefficients of Schiff base and its complex with CT-DNA, respectively. The plots of $A_0/(A-A_0)$ *versus* $[CT\text{-}DNA]^{-1}$ were linear (Figs. 13 and 14) and the K values were calculated from the ratio of the intercept to the slope (Table 5).
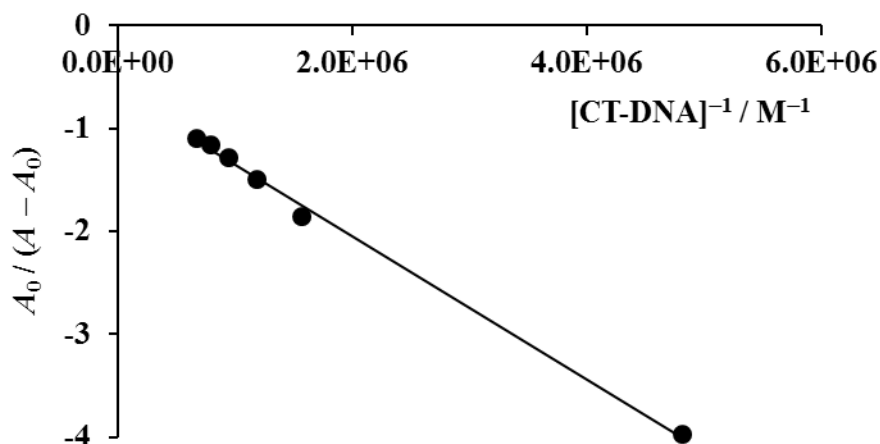
Figure 13. The plot of $A_0/(A - A_0)$ *versus* $[CT\text{-}DNA]^{-1}$ for Schiff base A. *Experimental conditions:* 8.34×10^{-5} M Schiff base A in 0.02 M phosphate buffer (pH 7.4) (the absorbances are read at 260 nm).
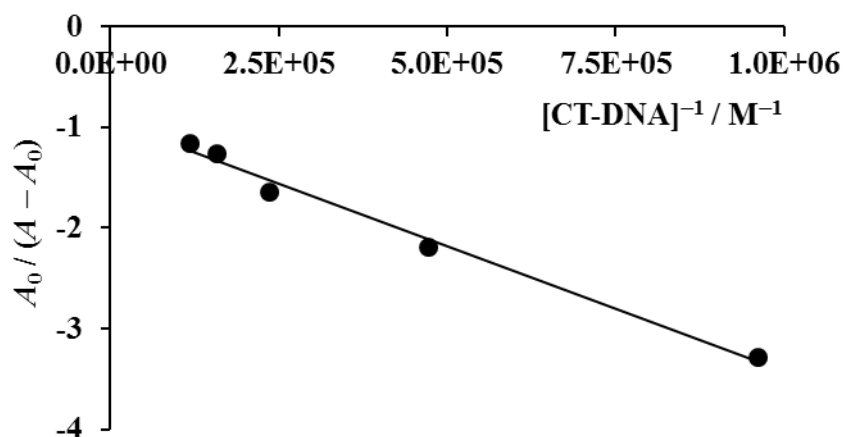

Figure 14. The plot of $A_0/(A - A_0)$ *versus* $[CT\text{-}DNA]^{-1}$ for Schiff base B. *Experimental conditions:* 4.17×10^{-4} M Schiff base B in 0.02 M phosphate buffer (pH 7.4) (the absorbances are read at 258 nm).

As can be seen in Table 5, the binding constant of Schiff base A is bigger than that of Schiff base B. This result indicates that Schiff base A has a higher affinity than Schiff base B for CT-DNA. This case was supported from both CV and UV-Vis. data.

4. CONCLUSIONS

In the present study, Schiff bases have been synthesized from the reaction of SMTZ with 3-methoxy and 5-nitro derivatives of salicylaldehyde and their antibacterial activities have been investigated. In addition, at physiological pH, the binding interactions between Schiff bases and CT-

DNA have been studied using electrochemical and spectroscopic techniques. Voltammetric and Uv-vis. spectral changes have affirmed the formation of 1:1 association complexes between Schiff bases and CT-DNA. The experimental data revealed that Schiff base A (includes –OCH_3 group) interacts with CT-DNA through electrostatic binding mode, however Schiff base B (includes –NO_2 group) intercalate into the CT-DNA base. It was found that the order of their binding constants was Schiff base A > Schiff base B. On the other hand, Schiff base B showed the higher antibacterial activity against the gram positive bacterium *S. aureus* ATCC 25923 (MIC=0.5 µg mL^{-1}) as compared with Schiff base A and other reagents under investigation. Also, the Schiff bases exhibited anti-bacterial activity like SMTZ (MIC=8 µg mL^{-1}) against gram negative bacteria *E. coli* ATCC 25922 and SXT-R *E. coli*. As a result, our *in vitro* findings give important information about antibacterial effectiveness and CT-DNA interactions for helping at the determination of the pharmaceutical activities of the Schiff bases.

SUPPLEMENTARY MATERIALS
CCDC 1552126 and CCDC 1557898 contain the supplementary crystallographic data for this paper. These data can be obtained free of charge via http://www.ccdc.cam.ac.uk/conts/retrieving.html, (or from the Cambridge Crystallographic Data Centre, 12, Union Road, Cambridge CB2 1EZ, UK; fax: +44 1223 336033).

References

1. A. Gupta and A.K. Halve, *Int. J. Curr. Pharm. Res.*, 7 (2015) 17.
2. D.-A. Qin, X.-Q. Cai, Q. Miao, Z.-H. Wang and M.-L. Hu, *Int. J. Electrochem. Sci.*, 9 (2014) 1608.
3. M. Sadeghi, M. Bayat, S. Cheraghi, K. Yari, R. Heydari, S. Dehdashtian and M. Shamsipur, *Luminescence*, 31 (2016) 108.
4. F. Ahmadi and B. Jafari, *Electroanalysis*, 23 (2011) 675.
5. Z. Hussain, E. Yousif, A. Ahmed and A. Altaie, *Org. Med. Chem. Lett.*, 4 (2014) 1.
6. V.S. Sonnekar, W.N. Jadhav, S.A. Dake, S.G. Dhole, S.S. Narwade and R.P. Pawar, *Eur. Chem. Bull.*, 3 (2014) 792.
7. N.G. Ahmed and H.Y. Al-Hashimi, *Eur. Chem. Bull.*, 5 (2016) 88.
8. B. Anupama and C. Gyana Kumari, *International Journal of Research in Chemistry and Environment*, 3 (2013) 172.
9. N. Sohrabi, N. Rasouli and M. Kamkar, *Bull. Korean Chem. Soc.*, 35 (2014) 2523.
10. N. Rajendiran and J. Thulasidhasan, *International Letters of Chemistry, Physics and Astronomy*, 59 (2015) 170.
11. N. Iqbal, J. Iqbal and M. Imran, *J. Sci. Res. (Lahore)*, 39 (2009) 15.
12. I. Rama and R. Selvameena, *J. Chem. Sci.*, 127 (2015) 671.
13. R. Hämäläinen, M. Lehtinen and U. Turpeinen, *Arch. Pharm. (Weinheim)*, 319 (1986) 415.
14. R.C. Maurya, J. Chourasia, D. Rajak, B.A. Malik, J.M. Mir, N. Jain and S. Batalia, *Arab. J. Chem.*, 9 (2016) S1084.
15. T.N. Omar, *Iraqi J. Pharm. Sci.*, 16 (2007) 5.

16. S.S. Mohamed, A. Abo-baker, S.M. Bensaber, M.I. Jaeda and T. Almog, *Int. J. Pharm. Pharm. Sci.*, 5 (2013) 38.
17. J. Anandakumaran, M.L. Sundararajan, G. Ramasamy and T. Jeyakumar, *Can. Chem. Trans.*, 4 (2016) 328.
18. M.A. Neelakantan, M. Esakkiammal, S.S. Mariappan, J. Dharmaraja and T. Jeyakumar, *Indian J. Pharm. Sci.*, 72 (2010) 216.
19. B.A. Elsayed, A.A. Elhenawy and A.S.A. Sultanah, *International Journal of Chemistry and Materials Research*, 2 (2014) 1.
20. A.S. Abu-Khadra, R.S. Farag and A.E.-D.M. Abdel-Hady, *Am. J. Analyt. Chem.*, 7 (2016) 233.
21. S.P. Rao and S. Ahmad, *Orient. J. Chem.*, 25 (2009) 637.
22. Z. Hussain, M. Khalaf, H. Adil, D. Zageer, F. Hassan, S. Mohammed and E. Yousif, *Res. J. Pharm. Biol. Chem. Sci.*, 7 (2016) 1008.
23. S. Mondal, S.M. Mandal, T.K., Mondal and C. Sinha, *Spectrochim. Acta A*, 150 (2015) 268.
24. G. Vellaiswamy and S. Ramaswamy, *Int. J. Pharm. Pharm. Sci.*, 6 (2014) 487.
25. B. Jain, S. Malik, N. Sharma and S. Sharma, *Der Chemica Sinica*, 4 (2013) 40.
26. M.S.D. Thankachi and S. Suthakumari, *J. Chem. Pharm. Res.*, 5 (2013) 1467.
27. A. Athar, F. Khan, W. Ahmed, Z. Ul-Haq and Z. Khan, *American-Eurasian J. Agric. & Environ. Sci.*, 15 (2015) 63.
28. A. Subashini, M. Hemamalini, P.T. Muthiah, G. Bocelli and A. Cantoni, *J. Chem. Crystallogr.*, 39 (2009) 112.
29. J. Anandakumaran, M.L. Sundararajan, G. Ramasamy and T. Jeyakumar, *J. Chem. Pharm. Res.*, 8 (2016) 54.
30. S. Kumar, M.S. Niranjan, K.C. Chaluvaraju, C.M. Jamakhandi and K. Dayanand, *Journal of Current Pharmaceutical Research*, 1 (2010) 39.
31. S. Sonar, S. Vaidya, M. Bagal and T.K. Chondhekar, *Adv. Appl. Sci. Res.*, 7 (2016) 13.
32. W.A. Al-Masoudi, H.Y. Mahmood, R.M. Othman and W.M. Shaker, *Journal of Advances in Chemistry*, 12 (2016) 4009.
33. M. Lehtinen, *Annales Academiae Scientiarum Fennicae Series A II Chemica*, 194 (1981) 6.
34. M.N. Tahir, Z.H. Chohan, H.A. Shad and I.U. Khan, *Acta Cryst. Sect. E*, 64 (2008) o720.
35. S. Kodge, K.H. Shivprasad, V. Durg and A. Kodge, *Int. J. Pharm. Bio. Sci.*, 8 (2017) 183.
36. M.S.D. Thankachi and S. Suthakumari, *The International Journal of Science & Technoledge*, 4 (2016) 9.
37. Q. Wang, Y. Huang, J.-S. Zhang and X.-B. Yang, Bioinorg. Chem. Appl., 2014 (2014) 1.
38. N. Shahabadi, S. Kashanian and F. Darabi, *DNA Cell Biol.*, 28 (2009) 589.
39. C.M. da Silva, M.M. Silva, F.S. Reis, A. L.T.G. Ruiz, J.E. de Carvalho, J.C.C. Santos, I. M. Figueiredo, R.B. Alves, L.V. Modolo and Â. de Fátima, *J. Photochem. Photobiol. B: Biol.*, 172 (2017) 129.
40. M.H. Helal, Z.A. Al-mudaris, M.H. Al-douh, H. Osman, H.A. Wahab, B.O. Alnajjar, H.H. Abdallah and A.M.S. Abdul Majid, *Int. J. Oncol.*, 41 (2012) 504.
41. N. Selamat, L.Y. Heng, N.I. Hassan and N.H.A. Karim, *Malaysian J. Anal. Sci.*, 20 (2016) 111.
42. J. Bai, R.-H. Wang, Y. Qiao, A. Wang and C.-J. Fang, *Drug Des. Devel. Ther.*, 11 (2017) 2227.
43. D. Ajloo, S. Shabanpanah, B. Shafaatian, M. Ghadamgahi, Y. Alipour, T. Lashgarbolouki and A.A. Saboury, *Int. J. Biol. Macromol.*, 77 (2015) 193.
44. M.A. Rizvi, Y. Dangat, Z. Yaseen, V. Gupta and K.Z. Khan, *Croat. Chem. Acta*, 88 (2015) 289.
45. S. Shamim, S. Murtaza and M.F. Nazar, *J. Chem. Soc. Pak.*, 38 (2016) 494.
46. K. Suresh, V.S. Minkov, K.K. Namila, E. Derevyannikova, E. Losev, A. Nangia and E.V. Boldyreva, *Cryst. Growth Des.*, 15 (2015) 3498.
47. E. Borrás, G. Alzuet, J. Borrás, J. Server-Carrió, A. Castiñeiras, M. Liu-González and F. Sanz-Ruiz, *Polyhedron*, 19 (2000) 1859.
48. D. Omanović and M. Branica, *Croat. Chem. Acta*, 71 (1998) 421.

49. R. Hajian, E. Ekhlasi and R. Daneshvar, *E-J. Chem.*, 9 (2012) 1587.
50. G. Paramaguru, R.V. Solomon, P. Venuvanalingam and R. Renganathan, *J. Fluoresc.*, 21 (2011) 1887.
51. Stoe & Cie. X-AREA and X-RED. Stoe & Cie, Darmstadt, Germany, 2002.
52. G.M. Sheldrick, *Acta Cryst. Sect. A*, 71 (2015) 3.
53. G.M. Sheldrick, SHELXL-2016/6: Program for Crystal Structure Determination, University of Göttingen, Göttingen, Germany, 2016.
54. L.J. Farrugia, *J. Appl. Cryst.*, 45 (2012) 849.
55. A.L. Spek, *Acta Cryst. Sect. D*, 65 (2009) 148.
56. Clinical and Laboratory Standards Institute (CLSI). Reference method for broth dilution antifungal susceptibility testing of yeasts. 3rd ed., Wayne: Clinical and Laboratory Standards Institute; 2008 (Approved standard. M27-S3).
57. S. Çakır, M. Odabaşoğlu, E. Biçer and Z. Yazar, *J. Mol. Struct.*, 918 (2009) 81.
58. M.M. Ghoneim, E.M. Mabrouk, A.M. Hassanein, M.A. El-Attar and E.A. Hesham, *Cent. Eur. J. Chem.*, 5 (2007) 898.
59. S. Çakır and E. Biçer, *J. Iran. Chem. Soc.*, 7 (2010) 394.
60. S.M. Sabry, M.H. Barary, M.H. Abdel-Hay and T.S. Belal, *J. Pharmaceut. Biomed. Anal.*, 34 (2004) 509.
61. E. Coşkun and E. Biçer, *Erciyes University Journal of Institute of Science and Technology*, 30 (2014) 296.
62. S. Bellú, E. Hure, M. Trapé, M. Rizzotto, E. Sutich, M. Sigrist and V. Moreno, *Quím. Nova*, 26 (2003) 188.
63. T. Takamura-Enya, H. Suzuki and Y. Hisamatsu, *Mutagenesis*, 21 (2006) 399.
64. L. Otero, G. Aguirre, L. Boiani, A. Denicola, C. Rigol, C. Olea-Azar, J.D. Maya, A. Morello, M. González, D. Gambino and H. Cerecetto, *Eur. J. Med. Chem.*, 41 (2006) 1231.
65. J.E. Page, J.W. Smith and J.G. Waller, *J. Phys. Chem.*, 53 (1949) 545.
66. Y. Jiang, Y. Yuan, K. Wang, H. Li, C. Xu and X. Yang, *Int. J. Electrochem. Sci.*, 7 (2012) 10933.
67. A.A. Ensafi, R. Hajian and S. Ebrahimi, *J. Braz. Chem. Soc.*, 20 (2009) 266.
68. A. Shah, A. Rauf, A. Ullah, A. Munir, R. Qureshi, I. Ahmad, M.T. Soomro and Z.-U. Rehman, *J. Electrochem. Sci. Eng.,* 3 (2013) 19.
69. P.K. Brahman, R.A. Dar and K.S. Pitre, *J. Saudi Chem. Soc.*, 20 (2016) S236.
70. M.S. Ibrahim, H.S.M. Ibrahim, M.M. Kamal and Y.M. Temerk, *Academic Platform Journal of Engineering and Science - APJES*, 2 (2014) 1.
71. W. Sun, J. Han, Y. Ren and K. Jiao, *J. Braz. Chem. Soc.*, 17 (2006) 510.
72. Z. Yang, D. Zhang, H. Long and Y. Liu, *J. Electroanal. Chem.*, 624 (2008) 91.
73. X. Hu, K. Jiao, W. Sun and J.-Y. You, *Electroanalysis*, 18 (2006) 613.
74. M.T. Carter and A.J. Bard, *J. Am. Chem. Soc.*, 109 (1987) 7528.
75. M.T. Carter, M. Rodriguez and A.J. Bard, *J. Am. Chem. Soc.*, 111 (1989) 8901.
76. D.-W. Pang and H.D. Abruña, *Anal. Chem.*, 70 (1998) 3162.
77. L. Wang, H. Xiong, X. Zhang and S. Wang, *Electrochem. Commun.*, 11 (2009) 2129.
78. Y. Temerk and H. Ibrahim, *J. Electroanal. Chem.*, 736 (2015) 1.
79. A. Shah, M. Zaheer, R. Qureshi, Z. Akhter and M.F. Nazar, *Spectrochim. Acta A*, 75 (2010) 1082.
80. K. Jiao, Q.-J. Li, W. Sun and Z.-J. Wang, *Electroanalysis*, 17 (2005) 997.
81. M. Mallappa, B.G. Gowda and R.T. Mahesh, *Der Pharma Chemica*, 6 (2014) 398.